Synthesis, structure and superconductivity in the $Ba_{1-x}K_xBiO_{3-y}$ system

D. G. Hinks, B. Dabrowski, J. D. Jorgensen, A. W. Mitchell, D. R. Richards, Shiyou Pei & Donglu Shi

Materials Science Division, Argonne National Laboratory, Argonne, Illinois 60439, USA

The recent discovery of superconductivity near 30 K in $Ba_{1-x}K_xBiO_{3-y}$ ($x \approx 0.4$)[1,2] is remarkable for two reasons. It is the first copper-free oxide superconductor that has a transition temperature (T_c) above that for the best intermetallic superconductor; and the structure is reported to be cubic, which excludes a two-dimensional metal–oxygen sublattice analogous to the CuO_2 planes believed to be responsible for superconductivity in the copper-oxide-based superconductors. Cava *et al.*[1] described a synthesis technique which involved starting with a 100% excess of KO_2. At least part of the excess potassium was found to be present in the final sample (in a form not detectable by X-ray diffraction), resulting in samples that were not suitable for resistivity measurements and making a precise determination of the potassium and oxygen content in the superconducting phase impossible. Here we describe a two-step synthesis technique starting with a stoichiometric oxide composition, which yields single-phase samples suitable for transport measurements. Neutron powder diffraction studies of samples with varying potassium concentration show that superconductivity in $Ba_{1-x}K_xBiO_{3-y}$ occurs only in a cubic perovskite phase which is stable at $\leqslant 600$ °C and which forms only for $x > 0.25$. Within this cubic phase, T_c is highest for compositions near the structural phase transition ($x \approx 0.25$) and decreases with increasing x.

Our initial attempts to synthesize $Ba_{1-x}K_xBiO_{3-y}$ in oxygen or air produced only mixtures of monoclinic $BaBiO_3$ (ref. 3) and monoclinic $KBiO_2$ (ref. 4); this, together with Cava *et al.*'s success[1] in synthesizing in sealed tubes, suggested that potassium might enter the compound only in an oxygen-deficient environment. For example, if the K must enter the compound without raising the average Bi charge above +4, then oxygen vacancies must be present during the high-temperature reaction; charge balance is maintained if 1/2 oxygen vacancy is formed for each K atom introduced. Based on this hypothesis, we developed a two-part synthesis technique in which a stoichiometric mixture of oxide powders is first reacted in an inert gas, to form the oxygen vacancies and allow the incorporation of K. A low-temperature oxygen anneal is then used to fill the oxygen vacancies without allowing diffusion of K from the lattice.

Stoichiometric mixtures of oxide powders were first reacted in flowing nitrogen at temperatures from 725 to 850 °C for 1 h. The maximum reaction temperature is limited by melting, but there is no evidence that one must anneal as close as possible to the melting temperature to achieve complete reactions; in fact, the best samples were reacted at 725 °C. This initial reaction produced a dark reddish-brown powder which was not superconducting. This powder was then annealed in flowing oxygen at temperatures from 475–675 °C for 30–60 min. Oxygen anneal temperatures of >550 °C or extended oxygen anneal times resulted in phase separation and non-superconducting samples (see below), whereas annealing at 475–550 °C resulted in a dark blue-black powder which was superconducting. Samples for neutron powder diffraction and a.c. susceptibility measurements were made as powders in batches of 2–10 g. For transport measurements, the reddish-brown powder was pressed into pellets before the final oxygen anneal.

Superconducting transition temperatures, T_c, were measured by both a.c. susceptibility and resistivity. The onset T_cs were the same for both the inductive and resistive measurements.

Table 1 Starting composition, oxygen anneal temperature, T_c, refined structural parameters for the cubic phase, and phases present in samples of $Ba_{1-x}K_xBiO_{3-y}$

x (init.)	T_{anneal} (°C)	T_c (K)	a (Å)	x (ref.)	y (ref.)	Phases*
0.20	550	0	4.3236 (1)			B
0.33	675	0	4.3186 (1)			B+D
0.33	550	27.1	4.3034 (1)	0.25 (3)	0.00 (2)	A+B
0.40	550	27.1	4.2932 (1)	0.29 (3)	0.02 (2)	A
0.40	475	21.4	4.2873 (1)	0.26 (4)	0.07 (3)	A
0.50	675	0	4.3173 (3)			B+C+D
0.50	550	22.6	4.2802 (1)	0.35 (3)	0.04 (2)	A+C+D
0.50	475	15.6	4.2745 (1)	0.40 (3)	0.03 (2)	A+C+D

Refinements are based on model 1 described in Table 2. Numbers in parentheses are standard deviations of the last significant digit. For the non-superconducting phase of $Ba_{1-x}K_xBiO_{3-y}$ for $x < 0.25$ (phase B), Rietveld refinement gives a pseudo-cubic lattice parameter but cannot yield values for x and y.

*Phases present are: A, $Ba_{1-x}K_xBiO_{3-y}$ ($x > 0.25$), cubic, superconducting; B, $Ba_{1-x}K_xBiO_{3-y}$ ($x < 0.25$), $z = 4$ supercell, non-superconducting (see text); C, $BaBiO_3$, monoclinic[3]; D, $KBiO_2$, monoclinic[4].

Typical resistive transitions were 3 °C wide; inductive transition widths varied from 3 to 6 °C in a random way. The magnitude of the change in susceptibility at T_c was compared with that measured for a reference sample of $La_{1.85}Sr_{0.15}CuO_4$. For all the superconducting samples the diamagnetic signal was as large or larger than that for the reference sample, thus confirming bulk superconductivity. The inductively measured onset T_cs for samples of differing starting compositions and oxygen anneal temperatures are listed in Table 1.

Neutron powder diffraction data were collected on the Special Environment Powder Diffractometer at the Intense Pulsed Neutron Source in runs of ~2 h per sample. For each sample, the phases were identified and the cubic lattice parameter and chemical composition (x and y) of the superconducting phase were determined by Rietveld refinement. The neutron diffraction results are summarized in Table 1. For samples where more than one phase was present, the minor impurity phases were included in the refinement with only their scale factors and lattice parameters being refined, to improve the precision of the refined parameters for the superconducting phase. Neutron powder diffraction was also used to examine the reddish-brown powder produced in the initial nitrogen anneal. In this way it was possible to determine if all of the initial K was present in the final superconducting phase, and, if not, whether it failed to

Table 2 Refined structural parameters for $Ba_{1-x}K_xBiO_{3-y}$ with an initial composition of $x = 0.4$ annealed in oxygen at 550 °C

		Model 1	Model 2
a (Å)		4.2932 (1)	4.2932 (1)
Ba site:	n(Ba)	0.71 (3)	0.618
	n(K)	0.29 (3)	0.35 (2)
	n(Bi)	0	0.030 (8)
	B (Å^2)	1.06 (5)	1.06 (5)
Bi site:	n(Bi)	1.00	1.000 (8)
	B (Å^2)	0.39 (3)	0.39 (3)
O site:	n(O)	2.98 (2)	2.98 (2)
	U_{11}^2 (Å^2)	0.0275 (6)	0.0277 (6)
	U_{33}^2 (Å^2)	0.0058 (6)	0.0059 (6)
	R_{wp}	0.0831	0.0828
	R_{exp}	0.0682	0.0682

Refinements are done in the cubic space group $Pm3m$ with Ba at (0, 0, 0), Bi at ($\frac{1}{2}$, $\frac{1}{2}$, $\frac{1}{2}$) and O at ($\frac{1}{2}$, $\frac{1}{2}$, 0). Model 1 allows only Ba or K on the Ba site. Model 2 allows anti-site defects on the Ba site; that is, Ba, K, or Bi on the Ba site and no defects on the Bi site, with the Ba : Bi ratio constrained at the starting composition. Numbers in parentheses are standard deviations of the last significant digit. Parameters with no standard deviations were not refined. Refined structural parameters (site occupancies, n, isotropic temperature factors, B, components of the anisotropic temperature factor, U_{ii}^2, weighted profile R value, R_{wp} and expected R value, R_{exp}) for $Ba_{1-x}K_xBaO_{3-y}$.

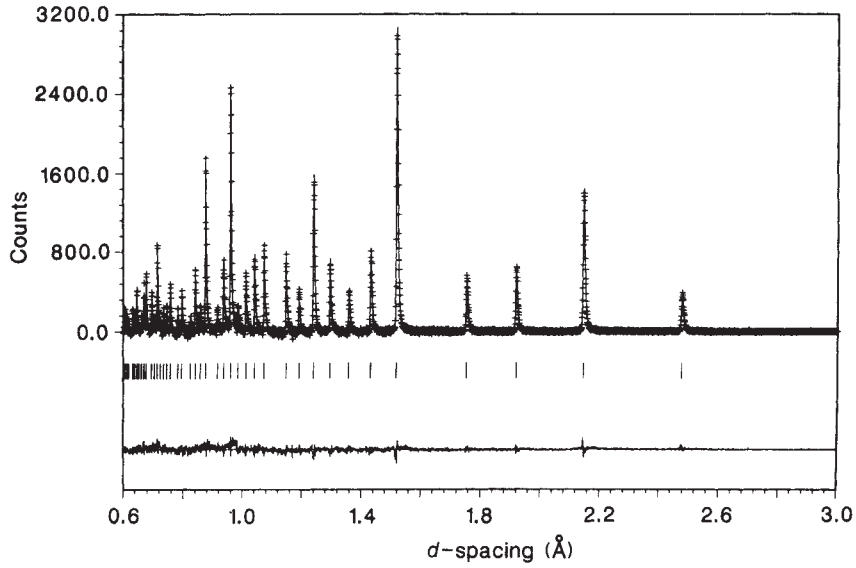

Fig. 1 Rietveld refinement profile for the cubic ($Pm3m$) superconducting sample of $Ba_{1-x}K_xBiO_{3-y}$ with starting composition $x = 0.4$, oxygen-annealed at 550 °C. Plus marks (+) are the raw time-of-flight neutron diffraction data; the solid line is the calculated profile. Tick marks below the profile mark the positions of allowed Bragg reflections included in the calculation. A difference curve (observed minus calculated) is plotted at the bottom. Background was subtracted before plotting.

react during the initial nitrogen anneal or was lost during the oxygen anneal.

Cubic, single-phase, superconducting material with $T_c = 27.1$ K was produced for a starting composition of $x = 0.4$ annealed in oxygen at 550 °C. Table 2 lists the complete structural parameters for a Rietveld refinement of data from this sample (Model 1); the raw data and calculated Rietveld profile are shown in Fig. 1. The refinement yields a K composition, x, of 0.29(3), which is less than the starting value, but no crystalline impurity phases are visible in the diffraction data. This suggests either an error in the initial KO_2 stoichiometry (perhaps due to impurities such as carbonate or hydroxide), formation of a non-crystalline phase containing K, or the loss of some K by volatilization during the high-temperature reaction in flowing nitrogen. As shown in Table 1, this systematic discrepancy between the initial and refined K compositions is present in all of the samples for which the K concentration could be measured by neutron diffraction.

Assuming that the final sample is deficient only in K, the absence of a Bi-containing impurity phase in the diffraction data must also be explained. One possibility is that a small number of Bi atoms occupy the Ba site; such solid-solution defects are well documented in the parent compound $BaBiO_3$ (ref. 5). This alternative structural model has also been investigated by Rietveld refinement, by constraining the overall Ba:Bi ratio at the starting composition, to investigate the magnitude of the resulting systematic error. The results of such a refinement for the sample of starting composition $x = 0.4$, annealed at 550 °C, are listed in Table 2 (Model 2). This alternative refinement shows that the K deficiency indicated by the neutron diffraction data is much smaller if a small number (~3%) of Bi substitutional defects are allowed on the Ba site. From neutron diffraction alone it is impossible to tell which model is correct. As there is no corroborating evidence for the existence of anti-site defects, the following discussion will be based on the simpler model. Thus, a systematic error in the refined K concentration of the magnitude indicated (~0.05) may be present in these measurements.

From the results presented in Table 1, several important features of the structural and superconducting phase diagrams of the $Ba_{1-x}K_xBiO_{3-y}$ system are evident. Superconducting samples with the cubic perovskite structure are obtained only for compositions with $x > 0.25$. At lower values of x there is a structural transition to a phase which is not superconducting. The sample of initial composition $x = 0.2$, oxygen-annealed at 550 °C is composed entirely of this non-superconducting phase. The sample with initial composition $x = 0.33$ annealed at 550 °C contains both superconducting and non-superconducting phases, and thus provides a fortuitous indication of the composition at the phase transition: the refined value of x is 0.25(3) (based on model 1).

For the phase with $x < 0.25$ we observe a diffraction pattern which can be indexed on a $z = 4$ body-centred tetragonal (or degenerate orthorhombic) cell with $a \approx b = 6.117$ Å and $c = 8.647$ Å ($\sqrt{2}a \times \sqrt{2}a \times 2a$). This cell is similar to the $I2/m$ monoclinic cell of $BaBiO_3$ (which is pseudotetragonal)[3] or the $I4/mcm$ tetragonal cell of superconducting $BaPb_{1-x}Bi_xO_3$[6]. However, as of this writing, no complete model has been found for this phase which agrees with the observed intensities and we have made no detailed investigation of the BaK_xBiO_{3-y} phase diagram for $0 < x < 0.25$.

Both samples of starting composition $x = 0.4$ are single-phase, but the sample annealed at a lower temperature (475 °C) exhibits a lower T_c. The Rietveld refinement shows the presence of oxygen vacancies, which may explain the depressed T_c. A significant depression of T_c resulting from small oxygen vacancy concentrations has previously been reported for $BaPb_{1-x}Bi_xO_{3-y}$[7], but an increased concentration of anti-site defects (Bi on the Ba site) might also be the cause.

Samples with starting composition $x = 0.5$ exhibit superconductivity but are not single-phase (see Table 1), suggesting that $x \approx 0.4$ is the solubility limit for K in this system under these synthesis conditions. This conclusion is consistent with ref. 1, in which samples of final compositions near $x = 0.4$ were produced from starting mixtures containing a 100% excess of KO_2. Samples annealed in oxygen at 675 °C do not contain the cubic phase and are not superconducting for any starting composition, leading to the conclusion that the cubic, superconducting phase is not stable in oxygen above ~600 °C.

The relationship between structural and superconducting behaviour is summarized in Fig. 2. As shown in Fig. 2*A*, the cubic lattice parameter of the superconducting phase varies monotonically with K concentration. The extrapolation of this curve to larger lattice constants provides an estimate of the K concentration of the non-superconducting samples with $x < 0.25$. From the refined pseudo-cubic lattice parameters for these samples (Table 1), $x = 0.15$–0.18.

Figure 2*B* shows the variation of T_c with K concentration. T_c is highest adjacent to the structural transition to the non-superconducting phase at $x = 0.25$, and decreases with increasing x. This behaviour differs from that observed in $BaPb_{1-x}Bi_xO_{3-y}$, where T_c does not vary with x within the superconducting phase (near $x = 0.25$)[8]. Such behaviour suggests a possible relationship between the superconductivity and the mechanism that drives the phase transition. If the transition is driven by soft vibrational modes, the corresponding phonons

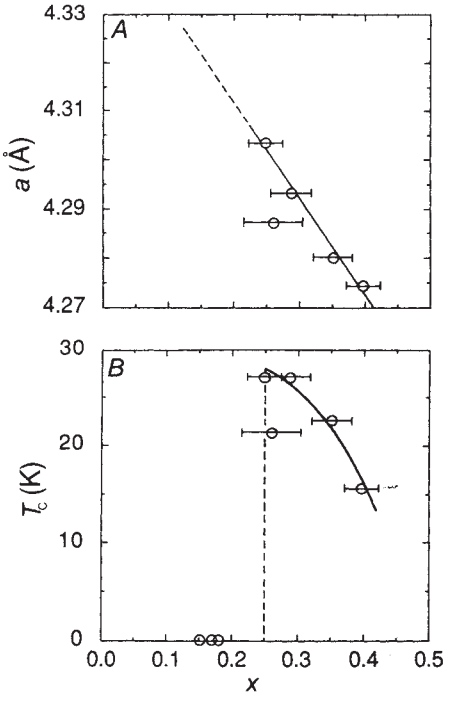

Fig. 2 Cubic lattice parameter (*A*) and superconducting transition temperature (*B*) of the superconducting phase of $Ba_{1-x}K_xBiO_{3-y}$ plotted against K concentration in the cubic, superconducting phase, *x*, as determined by Rietveld refinement of neutron powder diffraction data. The points at $x = 0.26$ which fall below the curves are for a sample in which oxygen vacancies are present. In *A*, the solid line fit to the remaining points is extended to larger values of *a* to allow the K concentration in non-superconducting samples with $x < 0.25$ to be estimated from the measured pseudo-cubic lattice parameter; these estimated concentrations are plotted on the *x*-axis in *B*.

may play an important role in the superconductivity. Alternatively, the transition may be electronically driven by a high density of electron states at the Fermi energy, in which case a lowering of the cell symmetry could open a gap at the Fermi energy, thereby lowering the free energy of the system. Such a 'band Jahn–Teller' transition occurs in the Chevrel-phase superconductors, giving rise to a transition from a metallic superconducting state to a semimetallic or semiconducting state which has been observed by varying pressure or composition. In the Chevrel-phase system, the highest T_cs are observed for compositions adjacent to this symmetry-lowering transition[9].

The high superconducting transition temperatures observed in the $Ba_{1-x}K_xBiO_{3-y}$ system, when compared with the lower T_cs (near 13 K) observed for $BaPb_{1-x}Bi_xO_3$, suggest that the integrity of the three-dimensional BiO_3 sublattice is important for obtaining the best superconductivity in this family of compounds. Thus, future efforts to optimize the superconducting properties of the $Ba_{1-x}K_xBiO_{3-y}$ system should concentrate on achieving a K concentration just above $x = 0.25$ and a minimum number of oxygen vacancies and anti-site defects, through careful control of the starting composition and the high-temperature nitrogen and low-temperature oxygen annealing conditions.

We thank Bruce Brown and the staff of the IPNS for providing an additional day of operation during the scheduled shut-down period expressly for these experiments. This work is supported by the US Dept of Energy, Basic Energy Sciences/Materials Sciences.

Received 1 June; accepted 14 June 1988.

1. Cava, R. J. *et al. Nature* **332**, 814–816 (1988).
2. Mattheiss, L. F., Gyorgy, E. M. & Johnson, D. W. Jr *Phys. Rev.* B **37**, 3745–3746 (1988).
3. Cox, D. E. & Sleight, A. W. *Solid St. Commun.* **19**, 969–973 (1976).
4. Schwedes, B. & Hoppe, R. *Z. anorg. allg. Chem.* **392**, 97–106 (1972).
5. Aurivillius, B. *Ark. Kemi Mineral. Geol.* **16A**, 1–13 (1943).
6. Cox, D. E. & Sleight, A. W. in *Proc. Conf. Neutron Scattering*, Gatlinburg, Tennessee, 45–54 (1976).
7. Suzuki, M. & Murakami, T. *Solid St. Commun.* **53**, 691–694 (1985).
8. Batlogg, B. *Physica* B**126**, 275–279 (1984).
9. Jorgensen, J. D., Hinks, D. G. & Felcher, G. P. *Phys. Rev.* B**35**, 5365–5368 (1987).

Efficiency of hydrothermal ore formation and the Panasqueira W–Cu(Ag)–Sn vein deposit

David A. Polya

Department of Geology, University of Manchester, Manchester M13 9PL, UK

Hydrothermal ore bodies are the concentrated manifestations of the large-scale mass transfer of ore-forming elements by aqueous fluids flowing through the Earth's crust. Existing mass transfer estimates[1–3] for hydrothermal ore-forming systems are based on ore reserve data, which do not take into account the mass of ore-forming elements dispersed in the metasomatized crust around the ore bodies. Here I report a method for the quantitative determination of this dispersed mass and hence the efficiency of ore formation. Application to the Panasqueira W–Cu(Ag)–Sn vein deposit in Portugal shows that only a few per cent of the hydrothermally introduced material (W, 33%; Cu, 8%; Sn, 3%; Zn, 1.5%) is concentrated in the ore body itself, implying that much greater volumes of ore-forming fluid are required than previously supposed. The efficiency of Panasqueira vein formation in concentrating these elements is variable, reflecting the relative importance of fluid pressure[4–6] and acid-consuming fluid/rock reactions[7] in determining different ore mineral solubilities, but it is broadly similar to the efficiency of sea-water mixing in immediately removing Pb and Zn from black smoker fluids[8].

The dispersion of ore-forming elements (OFEs) by hydrothermal fluids around many vein deposits[9] and in the Broadlands[10] and East Pacific Rise (21°N)[8,11] systems suggests that the dispersed mass of OFEs may be particularly important in the total mass transfer balance in and around hydrothermal ore bodies. Although there are numerous studies[12–18] of the spatial distribution of ore-forming components around ore deposits, there is an absence of data on the total mass of dispersed components in such haloes. This reflects the difficulty in simply transforming spatial distribution data to a total mass estimate. For a simple case, where the alteration envelope is a cylinder of height *h* and density ρ, the total dispersed mass of a component *i* is given by

$$M_i = \int_0^R \rho 2\pi r h [C_i(r) - C_i^U]\, dr \qquad (1)$$

where $C_i(r)$ is the mean concentration (w/w) of the component in the rock at a distance *r* from the centre of the ore body, C_i^U is the background concentration of the component in unaltered rock, and *R* is the radial extent of the alteration halo, typically several metres to several kilometres. Unfortunately, for most $C_i(r)$ functions, evaluation of the integral is particularly sensitive to changes in *R*, which in general cannot be determined with sufficient accuracy to meaningfully estimate M_i (see Fig. 1 for example). A method to overcome this problem is presented here and applied to a specific ore deposit.

The mass M_i of component *i* hydrothermally introduced into an alteration halo can be expressed by $M_i = \rho V F^A (C_i^A - C_i^U)$, where ρ is now the mean density of rock in the alteration halo, *V* its total volume, F^A the mean fraction of OFE-enriched hydrothermally altered rock in that volume, and C_i^A and C_i^U refer to the mean concentrations of component *i* in altered and unaltered rocks respectively.

For an isolated ore-forming hydrothermal system in a volume of isotropic crust, a normal distribution of the fraction F^A of